JACS
JOURNAL OF THE AMERICAN CHEMICAL SOCIETY

Communication

pubs.acs.org/JACS

Conjugated Cofactor Enables Efficient Temperature-Independent Electronic Transport Across ∼6 nm Long Halorhodopsin

Sabyasachi Mukhopadhyay,[†,‡] Sansa Dutta,[‡] Israel Pecht,[*,§] Mordechai Sheves,[*,‡] and David Cahen[*,†]

[†]Departments of Materials and Interfaces, [‡]Organic Chemistry, and [§]Immunology, Weizmann Institute of Science, Rehovot 76100, Israel

Supporting Information

ABSTRACT: We observe temperature-independent electron transport, characteristic of tunneling across a ∼6 nm thick Halorhodopsin (phR) monolayer. phR contains both retinal and a carotenoid, bacterioruberin, as cofactors, in a trimeric protein-chromophore complex. This finding is unusual because for conjugated oligo-imine molecular wires a transition from temperature-independent to -dependent electron transport, ETp, was reported at ∼4 nm wire length. In the ∼6 nm long phR, the ∼4 nm 50-carbon conjugated bacterioruberin is bound parallel to the α-helices of the peptide backbone. This places bacterioruberin's ends proximal to the two electrodes that contact the protein; thus, coupling to these electrodes may facilitate the activation-less current across the contacts. Oxidation of bacterioruberin eliminates its conjugation, causing the ETp to become temperature dependent (>180 K). Remarkably, even elimination of the retinal-protein covalent bond, with the fully conjugated bacterioruberin still present, leads to temperature-dependent ETp (>180 K). These results suggest that ETp via phR is cooperatively affected by both retinal and bacterioruberin cofactors.

Life of all organisms relies on electron transfer (ET), which is central to its energy conversion processes. Hence biological ET has been and is studied extensively with the aim of resolving its mechanism(s).[1] Biological ET is performed predominantly by proteins and generally relies on the presence of cofactors in them. These cofactors are usually metal ions or small conjugated molecules, bound to the protein, enabling its activities.[2,3] While nature has evolved a wide range of different electron transfer cofactors, diverse in structure and in their roles in protein functions, most of the cofactors in biological electron transfer chains are redox-active.[4] Studies of biological ET are normally carried out in environments that preserve the natural structure and activity of the studied protein.

With device integration of future bioelectronics in mind, it is of interest to explore solid state-like electron transport (ETp) via proteins.[5] ETp via proteins has been studied in single molecules (using scanning tunneling microscopy), or small ensembles of molecules (with conducting probe atomic force microscopy) and as macroscopic samples, all using (partial) protein monolayers on electronically conducting substrates.[6] Such measurements can complement electrochemical studies of ET via protein monolayers.[7] We study the temperature dependence of ETp via monolayers of several types of proteins, sandwiched between two electronically conducting, ionically blocking electrodes, in order to understand ETp mechanism(s). To this end also the roles of cofactors, their redox state, and their location, relative to the electrodes, were investigated.[6] One major question is to what extent ETp across protein monolayers is related to ET as the measured observables are similar to those of ET, where a rate (electrons/sec) is measured, while in ETp it is the electrical current (electrons/sec). In ETp this rate is normally measured as a function of a voltage (V), applied externally between two electrodes.

We found earlier that for Azurin (with copper ion as redox-active cofactor), human and bovine serum albumin (HSA and BSA) (without cofactor, as well as for HSA with artificially added cofactors), Cytochrome C (Cyt C, with heme as cofactor), and bacteriorhodopsin, bR (with retinal as cofactor), the presence of a cofactor markedly enhances the efficiency of ETp.[6] ETp across the protein−chromophore complex, Halorhodopsin (phR), is of interest because phR contains not only retinal as cofactor, as in bR, but also bacterioruberin, a ∼4 nm long carotenoid chromophore. The bacterioruberin is bound along the long axis of the protein, to crevices adjacent to protein subunits in the trimeric assembly (Figure 1).[8]

phR, which is isolated from the phR-overproducing mutant strain KM-1 of *Natronomonas pharaonis*, functions as a membranal light-driven chloride ion pump.[9] Its monomer is a seven-α helix transmembrane protein of the retinylidene protein family, homologous to the light-driven proton-pumping bacteriorhodopsin, both in secondary and tertiary, but not in its primary sequence structure.

Carotenoids, such as bacterioruberin (a polyene with 13 conjugated bonds), are an important group of pigments in bacteria, algae, and plant cells functioning as accessory light-harvesting pigments, strongly absorbing in the blue spectral region. The backbone of carotenoid chains contains double bonds that form a long conjugated π-electron system. Such carotenoids were found to be orders of magnitude better electronic conductors than alkanes.[6] The electrical conductance along the long axis of a single carotenoid polyene molecule was measured using the STM break-junction method and could be described by a small electron transfer decay constant ($\beta \approx 0.22$ Å^{-1}).[10] Transport through an 18-conjugated bonds polyene, inserted in an alkanethiol monolayer on a gold substrate, was also measured.[11] Analysis of the experimental results, combined with a theoretical study, showed that the single carotene molecule

Received: June 23, 2015
Published: August 24, 2015

DOI: 10.1021/jacs.5b06501
J. Am. Chem. Soc. 2015, 137, 11226−11229

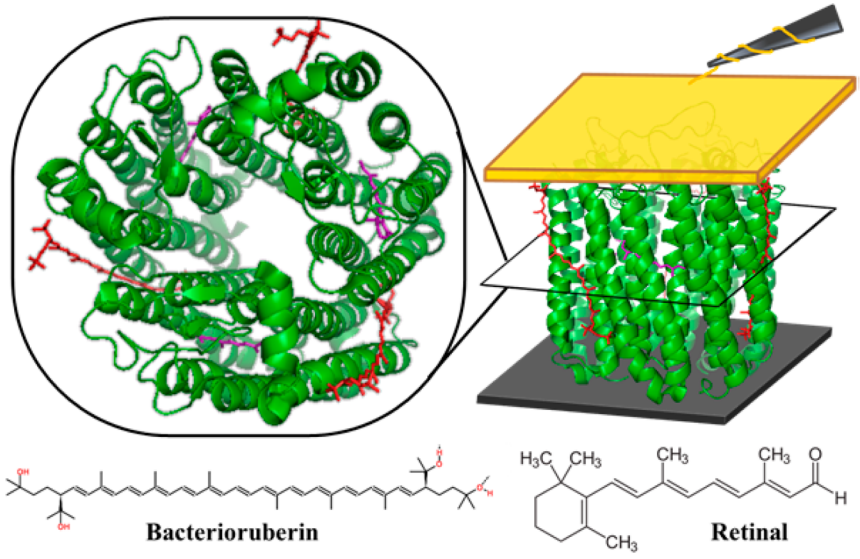

Figure 1. Three dimensional structure of phR (left) and a scheme of the two-electrode solid-state setup for ETp measurements, showing the conductive silicon substrate at the bottom, the top Au-LOFO contact, which in turn is contacted by a gold wire (diameter ≈ 25 μm), connected to the probe station (red-colored stick-rendering represents bacterioruberin and purple-colored stick-rendering represents retinal cofactor) (protein structures from protein data bank, PDB 3A7K). Bottom: Chemical structures of the phR cofactors.

conductance is largely due to electron tunneling through the conjugated chain.[11] Studies with α-aminoisobutyric acid-rich hexapeptides, constrained into a 3_{10}-helix and β-sheets, demonstrated that the presence of C═C bonds influences backbone rigidity and promotes electron transfer across the peptide.[12,13]

Solid-state electron transport measurements via different protein monolayers have shown that at room temperature (RT) ETp across bR is comparatively more efficient than across the globular proteins that we have measured so far, taking in account the differences in transport length across the protein.[6] In view of this, we examined whether Halorhodopsin (phR) as a homologue of bacteriorhodopsin (bR) might be even more efficient conductor, when immobilized with bacterioruberin oriented perpendicular to the electrodes (Figure 1, right, device scheme).

We have now prepared and measured ETp across phR monolayers, adsorbed on highly doped Si substrates where electronic junction formation was carried out as previously described.[5,14] In brief, controlled growth of ∼1 nm silicon oxide (SiO_x) on the highly doped p^{+2}-Si substrate provided a very smooth (rms roughness < ∼0.2 nm) surface onto which a monolayer of (3-aminopropyl)-trimethoxysilane (APTMS) was self-assembled to obtain a positively charged substrate. The protein was then electrostatically self-assembled onto the substrate by overnight incubation at 4 °C of a protein suspension (concentration of ∼1.6 μM; 100 mM NaCl). Use of a high salt concentration serves to retain the trimeric form of the protein during incubation.[8] Protein monolayers were characterized by atomic force microscopy (AFM), using the tapping mode and the nanoscratching method (Figure S4) to verify monolayer thickness (∼6 nm); ellipsometry yielded a thickness of 7−8.5 nm (the Protein Data Bank, 3A7K, crystal structure shows a ∼6 nm length along the long axis).[8,15] Linear dichroism measurements of the Halorhodopsin monolayers on a positively charged quartz surface showed that phR is immobilized with its long axis perpendicular to the electrodes (Figures S5 and S6), a conclusion, supported by electrostatic analyses (cf. section S7).

Room temperature transport measurements were carried out with Hg as top electrode. Measurements over different parts of the monolayer surface using different Hg drops showed that the phR monolayers are homogeneous on this scale (and allowed discarding the presence of pinhole), in terms of their electrical conduction; a set of results obtained over different batches of protein monolayers is given in the SI, Figure S7b [black trace with (current) error bars].

For temperature-dependence measurements of ETp we used, as top electrodes, ready-made Au pads, produced by thermal evaporation on a glass substrate, and then transferred from it by the Lift-Off Float-On, LOFO, method onto the phR monolayer. This protocol was used to avoid both possible thermal damage to the proteins and metal penetration through the monolayer, as are likely to occur with direct thermal evaporation.[14] The gold pad provided reproducible junction current−voltage ($I-V$) characteristics (four different samples with 2−3 LOFO contacts on each sample), when placed in a variable-temperature probe station (Lakeshore), evacuated to $\sim 10^{-5}$ mbar and equipped with down to fA resolution $I-V$ measurement electronics (Keithley 6430). The sample holder temperature was varied between 80 and 350 K with a Lakeshore 336 series temperature controller (∼0.2 K).

$I-V$ characteristics of a phR monolayer, immobilized on a Si substrate with LOFO as top electrode are illustrated in Figure S8. Current density (J, A/cm^2) across the phR monolayer, which was only ∼3 orders of magnitude lower than via the APTMS linker layer, exhibited negligible temperature dependence over the whole range (cf. Figure 2), in contrast to the clear temperature dependence >180 K, observed for bR monolayers.[14] In the linear $J-V$ regime (±50 mV) the nonmonotonous change in current densities over the examined temperature range is <40% (∼twice the maximum error in measurements); this is similar to and only slightly larger than that observed earlier for holo-azurin (holo-Az) monolayers, which also showed temperature-independent ETp.[16]

All of the proteins that have been studied so far (holo/apo-bR, HSA, doped HSA, WT Cyt C, apo-Az, and other Az-derivatives) show temperature-dependent ETp; only the ∼3 nm thick holo-

DOI: 10.1021/jacs.5b06501
J. Am. Chem. Soc. 2015, 137, 11226−11229

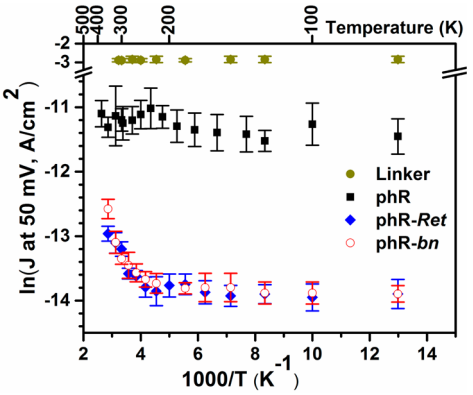

Figure 2. Arrhenius plot of the ETp via monolayers of Halorhodopsin (phR) and its different derivatives at +50 mV bias (phR-Ret corresponds to the product of phR treatment with hydroxylamine that cleaves the retinal−protein covalent bond. phR-bn corresponds to the bacterioruberin oxidation product, which lacks polyene conjugation. Error bars represent the deviations among different Au LOFO junctions during the heating cycle (80−350 K) for four different samples with 2−3 LOFO contacts on each sample. Figure S9a compares ETp efficiencies between Halorhodopsin and its derivatives with Azurin.

Az and recently the ∼7 nm thick photosystem I (PSI) proteins both gave temperature-independent ETp (cf. Figure S9a for holo-Az data).[14,16−19] Below 170−150 K, current is practically temperature independent, even sometimes slightly increasing with decreasing temperature. Above ∼200 K ETp becomes temperature dependent, with Arrhenius behavior over part of the temperature range, i.e., a linear $\ln(J)-1/T$ relation (cf. *phR-Ret*, *phR-bn* plots in Figure 2).[14,16]

In holo-Azurin, the proximity of Cu(II) and especially ligands of its first coordination shell that make physical contact to the electrode, may enhance the electronic coupling so as to allow tunneling transport across the ∼3 nm protein to dominate at all temperatures.[16] It is not as straightforward to use a proximity argument to rationalize tunneling across phR, which imposes a much wider, ∼6 nm separation between the electrodes. However, an obvious important difference between bR and phR is the presence of bacterioruberin in phR. Monolayer characterizations indicate its thickness is compatible only with positioning of the phR molecules with their long axis perpendicular to the substrate. Hence, the bacterioruberin will be placed roughly perpendicular to the two electrodes, spanning ∼4 nm of the ∼6 nm electrode gap and may well be critical for solid state ETp.[20]

Electronic transport that is essentially temperature-independent via any ∼6 nm long protein-chromophore is quite remarkable because the transition from temperature-independent to temperature-dependent transport via a model of conjugated oligo-imine wires was observed already at ∼4 nm molecular length.[21] Likely, electrodes−bacterioruberin electronic interactions facilitate efficient activation-less current flow across the contact interfaces. A possible mechanism is tunneling by superexchange between the protein terminals that contact the electrodes, and the polyene−bacterioruberin. Our observations pose an interesting question for future studies, i.e., is electrode-conjugated molecule coupling more efficient within a polypeptide matrix (as in our case) than without it (namely, by direct electrode contact of the conjugated molecules)?

The important role of the bacterioruberin and retinal in ETp was confirmed by *I*−*V* measurements on monolayers of Halorhodopsin derivatives as a function of temperature. Treatment of Halorhodopsin with $K_2S_2O_8$ oxidizes the bacterioruberin within the protein, eliminating the polyene conjugation that characterizes the carotenoid system, to yield *modified (bacterioruberin)*-phR [phR-*bn*] (cf. SI).[22,23] The oxidation was confirmed by the absence of bacterioruberin absorption peaks, both in solution and in the solid-state layer (Figure S1b). The maintenance of the chemical functionality of the retinal cofactor in *phR-bn* was affirmed by preservation of the retinal absorption peak at ∼570 nm (Figure S1b). The protein's secondary structure is preserved after the harsh chemical treatment as confirmed by the circular dichroism (CD) spectra of the phR-*bn* in solution where the native α-helix signature was observed (Figure S1a). Room temperature ETp measurements via phR-*bn* protein monolayers show ∼10 times lower currents than via phR at low applied bias (blue trace with current error bars in Figure S7b). More striking is that the phR-*bn* monolayer shows thermally activated transport at temperatures above 180 K and temperature-independent transport at lower temperatures (Figure 2).

To explore the role of the retinal cofactor, the structure of the retinal-contacting pocket and its contribution to ETp across a Halorhodopsin monolayer, a phR derivative was prepared with retinal oxime, *modified(retinal)*-phR [phR-*Ret*]. phR-*Ret* samples were obtained by treating phR with hydroxylamine (pH 7.2) to sever the retinal−protein covalent bond, where the resulting retinal oxime remains noncovalently bound within the protein. Consistent bacterioruberin absorption peaks and the high retinal reconstituted yield (∼80%) of phR-*Ret* upon incubation with all-*trans* retinal suggest that hydroxylamine does not react with the bacterioruberin and that the protein's structure and natural functionality of the retinal binding site are unaltered.[23]

Another, different modification of phR yielded *modified (retinal) (bacterioruberin)*-phR [phR-(*Ret*, *bn*)]. This was done by sequentially oxidizing bacterioruberin by $K_2S_2O_8$, followed by hydroxylamine treatment. This protocol alters both the bacterioruberin and the retinal cofactors of Halorhodopsin, sequentially. While CD spectra of phR-(*Ret*, *bn*) indicate conservation of the α-helical protein secondary structure (Figure S1a), only ∼40% reconstitution of phR-(*bn*) was obtained upon incubation of phR-(*Ret*, *bn*) with retinal, which may suggest that part of the protein conformation was changed by these chemical treatments.[23] Room temperature ETp measurements showed moderate ETp efficiency via phR-*Ret*, intermediate between those of phR and phR-*bn* monolayers, with a further decrease for phR=(*Ret*, *bn*) (cf. Figure S7b inset).

phR-*Ret* monolayers show temperature-dependent ETp above 180 K, similar to that of phR-*bn* (Figure 2). We also found temperature-dependent transport over the examined temperature range for phR=(*Ret*, *bn*) (Figure S9). Likely lower currents and weaker temperature dependence via phR-(*Ret*, *bn*) than via phR-*Ret* and phR-*bn* (Figures S7b and S9) indicate that the protein has partially denatured (consistent with the lower retinal reconstitution percentage).

Notwithstanding the likely role of the conjugated bacterioruberins in the tunneling even at high temperature across phR, we note that its presence is insufficient by itself, as in phR-*Ret*, with the bacterioruberin intact in place; we observe thermally activated transport at higher temperatures. This result indicates that the retinal, bound to its binding site in the peptide matrix, also plays a role in the ETp. Possibly, a change in protein conformation as a result of the chemical treatment that breaks the Schiff base bond and transforms the retinal into retinal oxime

DOI: 10.1021/jacs.5b06501
J. Am. Chem. Soc. 2015, 137, 11226−11229

decreases the efficiency of the transport pathway so that an alternative, thermally activated path now is more efficient at sufficiently high temperature.

phR-*Ret* monolayer demonstrates lower contribution of the bacterioruberin absorption band and sharpening of the amide-II peak (N−H stretching frequency, reflecting backbone peptide orientation in the protein), suggesting a minor conformation change upon retinal hydroxylamine formation (cf. Figures S1b and S2). At low bias, current density across phR-(*Ret*, *bn*) monolayers is ∼10 times lower compared to the other *modified*-phR derivatives (Figure S7b), and a weak monotonic increase in ETp is observed over the complete temperature range (Figure S9a). This result suggests that ETp across phR-(*Ret*, *bn*) monolayers, i.e., along partially conformational modified protein, is mostly an inefficient, weakly temperature-activated process.

In contrast to bacteriorhodopsin (bR) where ETp increases dramatically above 300 K, this increase is not seen for phR, and there might even be a minor drop in ETp efficiency >300 K (cf. Figure 2).[14] This might be due to a small change in the protein's native structure, analogous to more pronounced behavior of this type, seen for bR at low temperatures.[14]

Our experiments establish that ETp across Halorhodopsin monolayers is temperature independent and that its cofactors, retinal and bacterioruberin, play important roles in this process. The change in ETp upon modifying either the bacterioruberin or the retinal (and its interactions with the protein) indicates the coexistence of multiple transport pathways across this protein.[14] While it is tempting to ascribe the ETp temperature-independence only to the presence of the long polyene, results of phR-*Ret* show that the retinal also plays a role. Possibly, further insights may be obtained from studies of the Gloeobacter Rhodopsin−Salinixanthin complex, which shows efficient fluorescence resonance energy transfer from bacterioruberin to retinal, suggesting a closer proximity between these two chromophores than in phR.[24]

■ ASSOCIATED CONTENT

Supporting Information

The Supporting Information is available free of charge on the ACS Publications website at DOI: 10.1021/jacs.5b06501.

Detailed preparations and characterizations of phR and *modified*-phR derivatives proteins; linear dichroism measurements for protein orientation on substrate; spectroscopic and electrical characterization of proteins monolayers (PDF)

■ AUTHOR INFORMATION

Corresponding Authors

*israel.pecht@weizmann.ac.il
*mudi.sheves@weizmann.ac.il
*david.cahen@weizmann.ac.il

Notes

The authors declare no competing financial interest.

■ ACKNOWLEDGMENTS

We thank Dr. Noga Friedman, Dr. Michal Lahav, Noga Meir, and Prof. Dan Oron for their help with optical absorption measurements. We are grateful to the Minerva Foundation (Munich), the Nancy and Stephen Grand Centre for Sensors and Security, the Kimmelman Center for Biomolecular Structure and Assembly, the Benoziyo Endowment Fund for the Advancement of Science, and J & R Center for Scientific Research for partial support. S.M. thanks the Council for Higher Education (Israel) for a postdoctoral research fellowship. M.S. holds the Katzir−Makineni chair in Chemistry, and D.C. holds the Schaefer Chair in Energy Research.

■ REFERENCES

(1) Gray, H. B.; Winkler, J. R. *Q. Rev. Biophys.* **2003**, *36*, 341.
(2) Gray, H. B.; Winkler, J. R. *Annu. Rev. Biochem.* **1996**, *65*, 537.
(3) Beratan, D. N.; Liu, C.; Migliore, A.; Polizzi, N. F.; Skourtis, S. S.; Zhang, P.; Zhang, Y. *Acc. Chem. Res.* **2015**, *48*, 474.
(4) Page, C. C.; Moser, C. C.; Dutton, P. L. *Curr. Opin. Chem. Biol.* **2003**, *7*, 551.
(5) Ron, I.; Sepunaru, L.; Itzhakov, S.; Belenkova, T.; Friedman, N.; Pecht, I.; Sheves, M.; Cahen, D. *J. Am. Chem. Soc.* **2010**, *132*, 4131.
(6) Amdursky, N.; Marchak, D.; Sepunaru, L.; Pecht, I.; Sheves, M.; Cahen, D. *Adv. Mater.* **2014**, *26*, 7142.
(7) Moser, C. C.; Dutton, P. L. *Biochim. Biophys. Acta, Bioenerg.* **1992**, *1101*, 171.
(8) Kouyama, T.; Kanada, S.; Takeguchi, Y.; Narusawa, A.; Murakami, M.; Ihara, K. *J. Mol. Biol.* **2010**, *396*, 564.
(9) Ihara, K.; Narusawa, A.; Maruyama, K.; Takeguchi, M.; Kouyama, T. *FEBS Lett.* **2008**, *582*, 2931.
(10) He, J.; Chen, F.; Li, J.; Sankey, O. F.; Terazono, Y.; Herrero, C.; Gust, D.; Moore, T. A.; Moore, A. L.; Lindsay, S. M. *J. Am. Chem. Soc.* **2005**, *127*, 1384.
(11) Ramachandran, G. K.; Tomfohr, J. K.; Li, J.; Sankey, O. F.; Zarate, X.; Primak, A.; Terazono, Y.; Moore, T. A.; Moore, A. L.; Gust, D.; Nagahara, L. A.; Lindsay, S. M. *J. Phys. Chem. B* **2003**, *107*, 6162.
(12) Yu, J.; Zvarec, O.; Huang, D. M.; Bissett, M. A.; Scanlon, D. B.; Shapter, J. G.; Abell, A. D. *Chem. Commun.* **2012**, *48*, 1132.
(13) Horsley, J. R.; Yu, J.; Moore, K. E.; Shapter, J. G.; Abell, A. D. *J. Am. Chem. Soc.* **2014**, *136*, 12479.
(14) Sepunaru, L.; Friedman, N.; Pecht, I.; Sheves, M.; Cahen, D. *J. Am. Chem. Soc.* **2012**, *134*, 4169.
(15) Deviation between measured monolayer thickness from crystallographic data was also observed earlier with Azurin, and we assume this artifact mostly originates from optical absorption of protein monolayer (ref 5).
(16) Sepunaru, L.; Pecht, I.; Sheves, M.; Cahen, D. *J. Am. Chem. Soc.* **2011**, *133*, 2421.
(17) Castaneda Ocampo, O. E.; Gordiichuk, P.; Catarci, S.; Gautier, D. A.; Herrmann, A.; Chiechi, R. C. *J. Am. Chem. Soc.* **2015**, *137*, 8419.
(18) Amdursky, N.; Pecht, I.; Sheves, M.; Cahen, D. *J. Am. Chem. Soc.* **2012**, *134*, 18221.
(19) Amdursky, N.; Pecht, I.; Sheves, M.; Cahen, D. *J. Am. Chem. Soc.* **2013**, *135*, 6300.
(20) Sedghi, G.; Garcia-Suarez, V. M.; Esdaile, L. J.; Anderson, H. L.; Lambert, C. J.; Martin, S.; Bethell, D.; Higgins, S. J.; Elliott, M.; Bennett, N.; Macdonald, J. E.; Nichols, R. J. *Nat. Nanotechnol.* **2011**, *6*, 517.
(21) Choi, S. H.; Risko, C.; Delgado, M. C. R.; Kim, B.; Brédas, J.-L.; Frisbie, C. D. *J. Am. Chem. Soc.* **2010**, *132*, 4358.
(22) Imasheva, E.; Balashov, S.; Wang, J.; Lanyi, J. *J. Membr. Biol.* **2011**, *239*, 95.
(23) Dutta, S.; Weiner, L.; Sheves, M. *Biochemistry* **2015**, *54*, 3164.
(24) Iyer, E. S. S.; Gdor, I.; Eliash, T.; Sheves, M.; Ruhman, S. *J. Phys. Chem. B* **2015**, *119*, 2345.

DOI: 10.1021/jacs.5b06501
J. Am. Chem. Soc. 2015, 137, 11226−11229